Irrigation Science (2018) 36:187–201
https://doi.org/10.1007/s00271-018-0574-z

ORIGINAL PAPER

Improved soil water deficit estimation through the integration of canopy temperature measurements into a soil water balance model

Ming Han[1,2] · Huihui Zhang[1] · José L. Chávez[2] · Liwang Ma[3] · Thomas J. Trout[1] · Kendall C. DeJonge[1]

Received: 3 February 2017 / Accepted: 23 March 2018 / Published online: 4 April 2018

Abstract

The total available water in the soil root zone (TAW_r), which regulates the plant transpiration, is a critical parameter for irrigation management and hydrologic modeling studies. However, the TAW_r was not well-investigated in current hydrologic or agricultural research for two reasons: (1) there is no direct measurement method of this parameter; and (2) there is, in general, a large spatial and temporal variability of TAW_r. In this study, we propose a framework to improve TAW_r estimation by incorporating the crop water stress index (CWSI) from canopy temperature into the Food and Agriculture Organization of the United Nations (FAO) paper 56 water balance model. Field experiments of irrigation management were conducted for maize during the 2012, 2013 and 2015 growing seasons near Greeley, Colorado, USA. The performance of the FAO water balance model with CWSI-determined TAW_r was validated using measured soil water deficit. The statistical analyses between modeled and observed soil water deficit indicated that the CWSI-determined TAW_r significantly improved the performance of the soil water balance model, with reduction of the mean absolute error (MAE) and root mean squared error (RMSE) by 17 and 20%, respectively, compared with the standard FAO model (with experience estimated TAW_r). The proposed procedure may not work under well-watered conditions, because TAW_r may not influence the crop transpiration or crop water stress in both daily and seasonal scales under such conditions. The proposed procedure potentially could be applied in other ecosystems and with other crop water stress related measurements, such as surface evapotranspiration from remote sensing methodology.

Introduction

The agriculture sector is the major water consumer of limited fresh water resources. Thus, efficient agricultural water use is critical to improve irrigation water management and sustain agricultural production. It is important to predict the root zone soil water deficit (SWD) accurately to maximize water use efficiency under limited irrigation water supplies (Fereres and Soriano 2007). In the past 30 years, the FAO-56 (Food and Agricultural Organization, Paper 56, Allen et al. 1998) dual crop coefficient approach, with a water balance model, has been one of the most common approaches for soil water deficit prediction as well as for irrigation scheduling (Allen et al. 1998; Jensen and Allen 2016; Pereira et al. 2002; Raes et al. 2006). Compared with other modeling approaches, this FAO method needs fewer data inputs and provides acceptable SWD estimation (Kite and Droogers 2000; Rallo et al. 2011).

The performance of the FAO-56 model depends on the accuracy in determining the in situ basal crop coefficient (K_{cb}) and total available water in the root zone (TAW_r) (Campos et al. 2016; Hsiao et al. 2009; Steduto et al. 2009). K_{cb} is defined as the ratio between potential (i.e., "unstressed") crop transpiration and reference evapotranspiration (ET_o). The TAW_r is the total water available for plant use in the root zone, and it is used to determine crop water stress in the case of deficient water and amount of deep percolation in the case of excess water. K_{cb} is mainly influenced by crop phenology, crop ground cover, crop variety, crop

Communicated by E. Fereres.

✉ Huihui Zhang
Huihui.Zhang@ars.usda.gov

[1] Water Management and Systems Research Unit, USDA-ARS, 2150 Centre Avenue, Bldg. D, STE 320, Fort Collins, CO 80526, USA

[2] Department of Civil and Environmental Engineering, Colorado State University, Campus Delivery 1372, Fort Collins, CO 80523, USA

[3] Rangeland Resources and Systems Research Unit, USDA-ARS, 2150 Centre Avenue, Bldg. D, Fort Collins, CO 80526, USA

Table 1 Total irrigation and precipitation amounts for each treatment in different growth stage

Treatment (%vegetative ET/%maturity ET)	Late vegetative stage			Reproductive stage			Maturity stage		
	2012	2013	2015	2012	2013	2015	2012	2013	2015[†]
TR1 (100/100)	305	228	242	169	127	139	181	254	200
TR2 (100/50)	302	228	242	152	122	113	47	165	34
TR3 (80/80)	245	180	203	168	128	131	145	217	147
TR4 (80/65)	245	181	203	163	128	121	68	196	88
TR5 (80/50)	243	180	–	160	128	–	44	165	–
TR6 (80/40)	243	180	202	158	128	133	41	137	1
TR7 (65/80)	200	136	161	173	149	134	136	217	160
TR8 (65/65)	199	136	161	167	149	135	68	196	70
TR9 (65/50)	197	136	161	165	150	135	56	165	25
TR10 (65/40)	197	136	161	164	150	137	41	138	1
TR11 (50/50)	157	101	130	173	158	136	57	165	25
TR12 (40/40)	129	83	117	169	158	136	41	137	1
TR13 (40/80)	–	–	116	–	–	134	–	–	150

En dash (–) indicates no treatment in that season

TR treatment

[†]In year 2015, TR5 was replaced by TR13

height, environmental conditions and management (Allen and Pereira 2009), while TAW_r is influenced by the crop root development, soil hydraulic properties and crop type (Campos et al. 2016). Both parameters (K_{cb} and TAW_r) have strong temporal and spatial variability and are difficult to be determined accurately.

With the development of real-time monitoring technology, it is possible to better estimate K_{cb} and TAW_r to improve the performance of the FAO-56 water balance model. Some researchers have found good relationships between K_{cb} and crop ground cover or vegetation indices (Allen and Pereira 2009; Bryla et al. 2010; Hunsaker et al. 2003, 2005; Neale et al. 1990; Trout et al. 2008). Using the K_{cb} calculated from ground crop cover or vegetation indices has improved the FAO-56 model in ET and SWD estimation (Er-Raki et al. 2007; Toureiro et al. 2017). Besides calculating K_{cb} directly, other studies have integrated the information from remote sensing (Irmak and Kamble 2009; Santos et al. 2008), such as using actual evapotranspiration (ET_a) estimated from remote sensing energy balance models into the FAO-56 model (Crow et al. 2008; Er-Raki et al. 2008; Geli 2012; Neale et al. 2012). However, in these studies, TAW_r was derived from the prior knowledge of root depth and soil moisture measurements. Fewer efforts were made to estimate TAW_r to improve SWD prediction in the FAO-56 model. Recently, crop water stress index (CWSI) from canopy temperature has been successfully applied as a direct crop water stress measurement to determine actual transpiration (Kullberg et al. 2016; Taghvaeian et al. 2014a; Zhang and Wang 2013). Assuming that canopy temperature-based CWSI is the best proxy of crop water stress, the development of TAW_r could be inversely estimated via an optimization procedure, which minimizes the difference between the crop water stress coefficient in the FAO-56 model (K_s) and CWSI. Thus, TAW_r can be estimated without the prior knowledge of rooting depth and soil hydraulic properties. The proposed approach is assumed to be closer to the true TAW_r value.

In this study, we propose a framework that incorporates CWSI from canopy temperature measurements into the FAO-56 model by inversely estimating TAW_r. The FAO-56 water balance model SWD, with estimated TAW_r, was then compared with SWD measurements from a 3-year irrigation study in Greeley, Colorado, USA.

Materials and methods

Field experiment

A field experiment was conducted on maize (*Zea mays* L.) at the United States Department of Agriculture—Agricultural Research Service (USDA-ARS) Limited Irrigation Research Farm (LIRF), in Greeley, Colorado, USA (40°26′57″N, 104°38′12″W, elevation 1427 m). The alluvial soils of the study field are predominantly sandy and fine sandy loam of Olney and Otero series. During the three seasons evaluated, maize was planted on 1 May, 15 May, and 1 Jun in 2012, 2013, and 2015, respectively. The plant density was 80,000–82,000 seeds ha^{-1}. During the three growing seasons, twelve levels of growth stage based deficit irrigation treatments (Table 1, Column 1) were arranged in a randomized block design with four replications. The crop was given adequate water to avoid stress during the early vegetative growth, for crop establishment, and during reproductive

Table 2 Average daily weather conditions during the growing season (from seeding to harvest) in 2012, 2013 and 2015

Year	T_{mean}	T_{max}	T_{min}	VPD	RH_{max}	RH_{min}	R_n	u_2	P
2012	20	30	11	1.06	0.88	0.19	23	175	124
2013	20	30	12	1.28	0.92	0.25	22	184	192
2015	19	28	8	1.24	0.96	0.25	20	144	129

T_{mean} is the mean daily temperature (°C), T_{max} is the maximum daily temperature (°C), T_{min} is the minimum daily temperature (°C), VPD is the vapor pressure deficit (kPa), RH_{max} is the maximum relative humidity (%), RH_{min} is the minimum relative humidity (%), u_2 is the daily averaged wind speed from 2 m height (km day^{-1}), R_n is the average daily net radiation (MJ m^{-2}); P is sum of the seasonal precipitation (mm)

growth to avoid significant yield loss. The deficit irrigation was applied during the late vegetative growth stage and/or the maturity growth stage. Each treatment targeted a percent of maximum non-stressed crop ET during late vegetative and maturity growth stages, respectively (e.g., 100/50 treatment would target 100% of maximum ET during the late vegetative stage and 50% of maximum ET during the maturity stage). Each treatment plot was 9 by 43 m with 12 rows at 0.76 m spacing. All the measurements were taken from the middle six rows to reduce border effects. Sum of actual irrigation amounts and precipitation for each treatment by growth stage are shown in Table 1. During the growing seasons, water was applied using 16 mm diameter drip irrigation tubing, which was placed next to each row of maize. Fertilizers were applied at planting and via chemigation to avoid nutrient deficiencies on all the treatments (DeJonge et al. 2015). Meteorological data were acquired by the on-site Colorado Agricultural Meteorological Network GLY04 weather station (CoAgMet, http://ccc.atmos.colostate.edu/~coagmet/). The measurements included hourly air temperature, relative humidity, incoming shortwave solar radiation, horizontal wind speed at 2 m above a grass reference surface, and daily precipitation. Seasonal average climate factors in each year were shown in Table 2.

Soil water content measurement

A neutron moisture meter (CPN-503 Hydroprobe, InstroTek, San Francisco, CA[1]) was used to measure SWC at depths of 300, 600, and 900 mm in the middle row (6th or 7th of 12) of each plot. SWC at the 0–150 mm layer was measured by a portable time domain reflectometer (MiniTrace, Soil moisture Equipment Corp, Santa Barbara, CA). The SWC measurements were taken two to three times a week, from middle of the vegetative stage to end of the crop growth season. Field capacity was estimated for each soil layer from SWC measurements following large irrigation or rainfall events, obtained during the field experiment since 2008. The SWC measured by neutron attenuation was assumed to represent the soil profile within 150 mm of the measurement depth (e.g., measurement taken at 300 mm was assumed as a homogeneous representation of the soil profile between depths of 150 and 450 mm). Because there was no evidence of water uptake from deeper soil layers, the observed SWD in each plot was calculated by adding soil water deficits from 0 to a depth of 1050 mm. More detailed information about soil water measurement and soil deficit calculation can be found in DeJonge et al. (2015).

Canopy temperature measurement

Canopy temperature of maize was continuously measured by thermal infrared radiometers (IRT, model: SI-121, Apogee Instruments, Inc., Logan, Utah, USA). The IRT measurement error (bias) was ±0.2 °C. IRTs were installed on a fixed stand and pointed in an oblique fashion to ensure viewing primarily crop canopy. The IRT angle was set 23° below the horizon and 45° from north (looking northeast). During the vegetative growth stage, the height of IRT was adjusted twice per week to keep it at 0.8 m above the top of the crop canopy. Treatments on which canopy temperature was measured each season are shown in Table 3. Averaged IRT measurements were recorded by data-loggers (model: CR1000, Campbell Scientific Inc., Logan, Utah, USA), on 30 min intervals. More details about IRT measurements and calibration could be found in (DeJonge et al. 2015).

IRT canopy temperature measurements and vapor pressure deficit (VPD) from Treatment 1 (fully irrigated) following irrigation events on 14, 21 and 11 sunny days in 2012, 2013 and 2015, were used to establish a non-stress baseline for maize. The canopy temperature, air temperature and VDP at 11:00, 12:00, 13:00 and 14:00 Mountain Standard Time (MST) from each selected day were used (Idso et al. 1981; Taghvaeian et al. 2014b). The net radiation and air temperature at 11:00, 12:00, 13:00 and 14:00 MST from each selected day were used to calculate the seasonal average net radiation and temperature. The seasonal average aerodynamic and potential canopy resistances were calculated based on the slope and intercept of the non-stress baseline, using Eqs. (23 and 24) (from "Appendix 1").

[1] Mention of trade names or commercial products in this publication is solely for the purpose of providing specific information and does not imply recommendation or endorsement by the U.S. Department of Agriculture.

Table 3 Treatments on which canopy temperature was measured in 2012, 2013, and 2015

Treatment (%vegetative ET/%maturity ET)	2012 6/20–9/3	2013 7/2–9/10	2015 7/14–9/20
TR1 (100/100)	x	x	x
TR2 (100/50)	x	x	x
TR3 (80/80)			x
TR4 (80/65)			
TR5 (80/50)			
TR6 (80/40)	x	x	
TR7 (65/80)			
TR8 (65/65)	x	x	x
TR9 (65/50)			x
TR10 (65/40)	x		x
TR11 (50/50)			x
TR12 (40/40)	x	x	x
TR13 (40/80)			x

Hourly CWSI values at 11:00, 12:00, 13:00, and 14:00 MST were calculated using Eq. (13) and the theoretical model in "Appendix 1" (Clawson et al. 1989; Jalali-Farahani et al. 1993) during the IRT measurement period for each year. Daily CWSI was then obtained by averaging the CWSI values over 4 h in each day. CWSI for each growth stage was calculated by average measured daily CWSI values in each growth stage.

Model and parameter determination

FAO-56 soil water balance model

According to Allen et al. (1998), the root zone soil water balance, at daily time steps, is given by the Eq. (1) below.

$$\mathrm{SWDr}_i = \mathrm{SWDr}_{i-1} + T_i + E_i + \mathrm{DP}_i - (P_i - \mathrm{RO}_i) - I_i - \mathrm{CR}_i, \quad (1)$$

where SWDr_i is the root zone soil water deficit on day i, SWDr_{i-1} is soil water deficit on day $i-1$, T_i is actual plant transpiration on day i, E_i is soil evaporation on day i, DP_i is deep water percolation from the root zone on day i, P_i and I_i are gross precipitation and net irrigation (that infiltrates into the soil), respectively, on day i, RO_i is the runoff from soil surface on day i, and CR_i is the capillarity rise from the ground water. The units of the above components are in mm day^{-1}.

In this study, we assumed there was no surface runoff (RO_i) in the field (drip irrigation system, low slope and moderately high soil infiltration, with no observed runoff events due to high rainfall), and the capillarity rise (CR_i) was assumed to be nonexistent considering the 6 m deep water table. The maximum effective maize root zone depth observed in this field was around 1.05 m (Comas et al. 2013).

The SWDr_i is limited by the total plant available water in the root zone, and the minimum value of SWDr_i is zero, when soil water content is at field capacity. Deep percolation only occurred when calculated SWDr_i is less than zero, following a large rain or irrigation event (projected soil water content (SWC) exceeds field capacity in the soil root zone). In this case, the SWDr_i will be reset to zero and the excess of water will be assigned to deep percolation (Allen et al. 1998).

According to Allen et al. (1998), actual transpiration (T_i) and actual soil evaporation (E_i) in Eq. (1) are determined by the dual coefficient method:

$$T_i = K_{\mathrm{s},i} \times K_{\mathrm{cb},i} \times \mathrm{ET}_{0,i}, \quad (2)$$

$$E_{\mathrm{s},i} = K_{\mathrm{e},i} \times ET_{0,i}, \quad (3)$$

where, $K_{\mathrm{s},i}$ is the water stress coefficient, which ranges from 0 to 1 and decreases crop transpiration based on soil water availability (more details in Sect. "Water stress coefficient, $K_{\mathrm{s,i}}$"). $K_{cb,i}$ is the basal crop coefficient, which is the ratio of crop potential transpiration to reference crop evapotranspiration. $\mathrm{ET}_{\mathrm{o},i}$ is the reference crop evapotranspiration (either alfalfa or grass, in this study is grass based) on day i, and $K_{\mathrm{e},i}$ is soil water evaporation coefficient on day i.

Water stress coefficient, $K_{\mathrm{s,i}}$

The water stress coefficient is affected by $\mathrm{TAW}_{\mathrm{r}}$, SWDr, and potential transpiration rate. Colaizzi et al. (2003) found that K_{s} determined by the approach (Eq. 4) suggested by Jensen et al. (1970) had a better correlation with CWSI than the K_{s} from the FAO-56 approach (Allen et al. 1998). Thus in this study, the K_{s} was defined as (Colaizzi et al. 2003; Jensen et al. 1970):

$$K_{\mathrm{s},i} = \frac{\ln[(1 - \mathrm{fDEP}_{i-1}) \times 100 + 1]}{\ln(101)}, \quad (4)$$

where the fDEP_{i-1} is the ratio of current root zone soil water deficit on day $i-1$ (SWDr_{i-1}) and root zone total available water on day i ($\mathrm{TAW}_{\mathrm{ri}}$):

$$\mathrm{fDEP}_{i-1} = \frac{\mathrm{SWD}_{\mathrm{r},i-1} + R\mathrm{IniDeep}_i}{\mathrm{TAWr}_i}, \quad (5)$$

where $\mathrm{RIniDeep}_i$ is the initial soil water deficit in deeper soil layers that does not affect plant transpiration at the beginning of simulation, before root system is developed.

At the beginning of the simulation, only the observed initial soil water deficit at the 0–150 mm depth was used in the soil water balance model. As roots develop, initial soil water deficit in the eventual root zone below the initial root

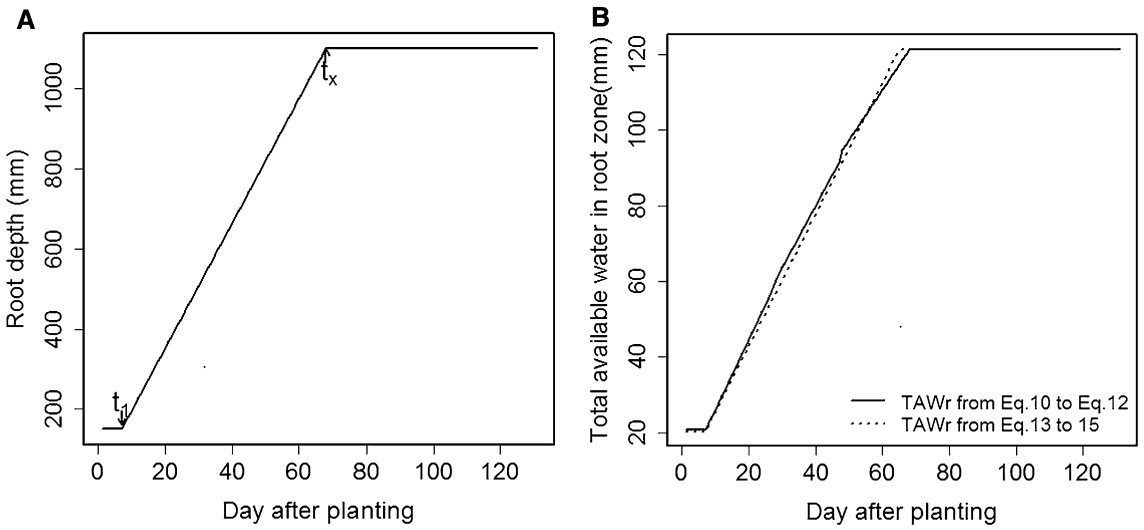

Fig. 1 Crop root development (**a**) and TAW_r development (**b**). TAW_r is the total available water in the root zone

zone (from 150 to 1050 mm) was linearly added to the soil water balance model as the increase of TAW_r, by:

$$RIniDeep_i = IniDeep \times \frac{TAWr_i - TAW_{min}}{TAW_{max} - TAW_{min}}, \quad (6)$$

where IniDeep is the observed initial soil water deficit in deeper soil layers (150–1050 mm in this study), TAW_{ri} is the current total available water in root zone for crop uptake. TAW_{min} is the minimum total available water in root zone, which is the value before root development. TAW_{max} is the maximum total root zone available water, when root reaches its maximum depth; more detailed explanations of TAW_{ri}, TAW_{min} and TAW_{max} are in Sect. "Total available water, TAW_r".

At the end of each day, IniDeep is reduced by the deep percolation from the root zone:

$$IniDeep = \max(IniDeep - DP_i, 0), \quad (7)$$

and DP_i is updated by:

$$DP_i = \max(DP_i - IniDeep, 0). \quad (8)$$

Total available water, TAW_r

The total available water in the root zone (TAW_r) is affected by soil texture and rooting depth, and is calculated by the following equation (Allen et al. 1998):

$$TAWr_i = (\theta_{FC} - \theta_{WP}) \times Z_{r,i}, \quad (9)$$

where θ_{FC} is the volumetric water content at field capacity (mm mm^{-1}), θ_{WP} is the soil volumetric water content at the wilting point (mm mm^{-1}), and Z_r is the effective rooting depth (mm).

By assuming a linear root zone increase during the growing season, the development of Z_r could be described by Steduto et al. (2009):

When $t_i < t_1$,

$$Z_{r,i} = Z_{min}. \quad (10)$$

When $t_1 < t_i < t_x$,

$$Z_{r,i} = Z_{min} + (Z_{max} - Z_{min}) \times \frac{t_i - t_1}{t_x - t_1}. \quad (11)$$

When $t_i > t_x$,

$$Z_{r,i} = Z_{max}, \quad (12)$$

where t_i is any day after planting, t_1 is the day after planting when effective rooting depth begins to increase from its minimum value (Z_{min}), and t_x is the day when effective root depth reaches its maximum (Z_{max}). The development of the effective root zone depth is shown in Fig. 1a.

Based on Eqs. 10–12, the development of TAW_r during the growing season was estimated and shown as a solid line in Fig. 1b. The dynamics of TAW_r was mainly controlled by the increase in the effective root zone depth; whereas the total plant available water, $\theta_{FC} - \theta_{WP}$, in each soil layer affects the rate of change the TAW_r (the solid line in Fig. 1b).

At least six parameters for each soil layer (t_1, t_x, Z_{min}, Z_{max}, and θ_{FC}, and θ_{WP}), and prior knowledge on soil texture, are needed to estimate TAW_r with the above procedure. In this paper, a new approach was proposed to determine the TAW_r instead of using Eqs. 10–12, and with fewer parameters and without the need of prior knowledge of soil properties:

When $t_i < t_1$.

$$\mathrm{TAWr}_i = \mathrm{TAW}_{\min}. \quad (13)$$

When $t_1 < t_i < t_x$

$$\mathrm{TAWr}_i = \mathrm{TAW}_{\min} + (\mathrm{TAW}_{\max} - \mathrm{TAW}_{\min}) \times \frac{t_i - t_1}{t_x - t_1}. \quad (14)$$

When $t_i > t_x$

$$\mathrm{TAWr}_i = \mathrm{TAW}_{\max}, \quad (15)$$

where $\mathrm{TAW}_{\min}$ is the minimum root zone soil total available water in mm and $\mathrm{TAW}_{\max}$ is the maximum root zone soil total available water in mm.

The TAW_r calculated from Eqs. (13–15) is shown as a dashed line in Fig. 1b, which is close to that estimated from Eqs. (10–12), but with only four parameters (t_1, t_x, $\mathrm{TAW}_{\min}$, $\mathrm{TAW}_{\max}$), and these four parameters will be estimated by an optimization procedure (Sect. "Inverse procedure for TAW_r estimation").

Evaporation and basal transpiration coefficients, K_e and K_{cb}

The estimation of evaporation coefficient (K_e) in Eq. (3) requires knowledge of the maximum soil evaporation depth (Z_e) and soil hydraulic properties (θ_{FC} and θ_{WP}) in the surface soil layer to determine the total available water for evaporation (similar to Eq. 9) (Allen et al. 1998). The maximum soil evaporation depth (Z_e) was assumed as 100 mm (Allen et al. 1998). As the seeding depth in this experiment is 50 mm, it is reasonable to assume that the effective rooting depth at the beginning of root development ($Z_{\min}$) is the same as the maximum soil evaporation depth (Z_e). Based on this assumption, total available water for soil evaporation was the same as total available water for crop transpiration ($\mathrm{TAW}_{\min}$). The K_{cb_mid}, K_{cb_ini}, and K_{cb_end} were obtained from the FAO-56 document ($K_{cb\_ini} = K_{cb\_end}$), and K_{cb_mid} was adjusted based on local climate (wind speed, relative humility and crop height) (Allen et al. 1998). When fractional canopy cover was larger than 0.8, $K_{cb,i}$ was equal with K_{cb_mid}, and when fractional canopy cover was smaller than 0.2, $K_{cb,i}$ was equal with $K_{cb\_ini} = K_{cb\_end}$, and when $K_{cb,i}$ ranged between 0.2 and 0.8, K_{cb} was linearly increased from K_{cb_ini} to K_{cb_mid} (Allen et al. 1998).

The calculation procedure of the water balance model is shown in Fig. 2.

CWSI to determine K_s

One of the widely used methods for estimating crop water stress index (CWSI) is based on measured canopy temperature (Idso 1981; Jackson et al. 1981, 1988).

CWSI is defined in Eq. 16 by the upper $(T_c - T_a)_u$ and lower boundary $(T_c - T_a)_l$ of temperature difference between the crop canopy and the air above it, where $(T_c - T_a)_u$ and $(T_c - T_a)_l$ represent non-transpiring and fully transpiring conditions, respectively (Idso et al. 1981; Jackson et al. 1981).

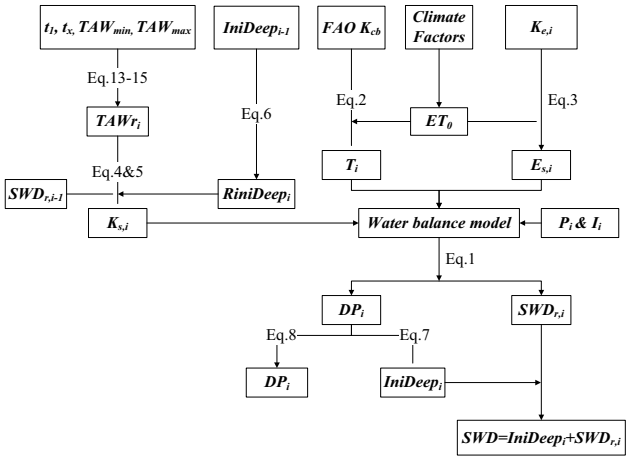

Fig. 2 FAO-56 water balance model calculation procedure

$$\mathrm{CWSI}_i = \frac{(T_c - T_a)_i - (T_c - T_a)_l}{(T_c - T_a)_u - (T_c - T_a)_l}, \quad (16)$$

where $(T_c - T_a)_i$ is the difference between canopy temperature (T_c, °C) and air temperature (T_a, °C) on day i. When a crop is under full soil–water condition or no water stress, the CWSI value is close to 0; while for a crop under severe water stress condition, CWSI is close to 1. A detailed calculation procedure for $(T_c - T_a)_u$ and $(T_c - T_a)_l$ can be found in "Appendix 1". To inversely calculate TAW_r through Eqs. (13, 14 and 15), the water stress coefficient (K_s_CWSI) from CWSI was determined as:

$$K_s\_\mathrm{CWSI}_i = (1 - \mathrm{CWSI}_i). \quad (17)$$

When CWSI = 0 then $K_s = 1$, there is no limitation on plant transpiration. However, as the value of CWSI approaches 1, then K_s will approach 0. In this case, the plant transpiration will shut down due to severe water stress.

Inverse procedure for TAW_r estimation

In the above soil water balance model, the unknown parameters are t_1, t_x, $\mathrm{TAW}_{\min}$, $\mathrm{TAW}_{\max}$ in Eqs. (13–15). The soil water balance model estimates the daily SWD_r, which can be used to estimate the daily water stress coefficient K_s for any given t_1, t_x, $\mathrm{TAW}_{\min}$, $\mathrm{TAW}_{\max}$. Alternatively, the CWSI stress coefficient (K_s_CWSI) can be calculated using Eq. 17 which integrates canopy temperature measurements. Therefore, an optimized procedure is proposed to estimate t_1, t_x, $\mathrm{TAW}_{\min}$, and $\mathrm{TAW}_{\max}$ by minimizing the difference between the K_s calculated from a soil water balance model and K_s_CWSI from canopy temperature measurements (Fig. 3).

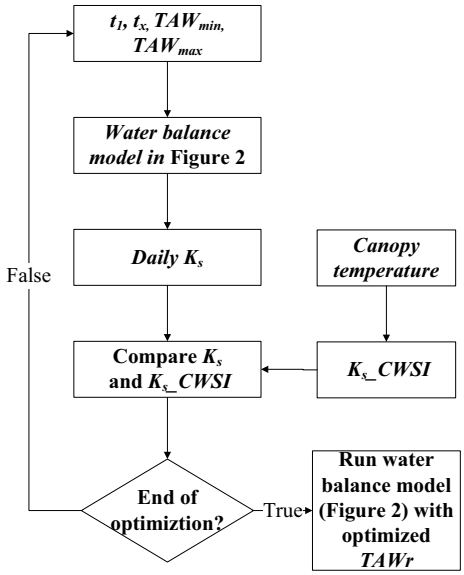

Fig. 3 The inverse procedure to determine TAWr from canopy temperature

First, the coefficient of determination (R^2) between K_s and K_s_CWSI was optimized. In the optimization, when R^2 (for the linear regression between K_s and K_s_CWSI) was larger than 0.5, the absolute difference (mean absolute error, MAE) between K_s and K_s_CWSI was minimized. The procedure was applied using a multi-objective optimization package (mco) in the statistical program R (Mersmann et al. 2014). The objective function was defined as follows (Mersmann et al. 2014):

When

$$R^2 = \frac{\sum_{i=1}^{n}(K_{s,i} - \bar{K}_{s,i})(K_s\_\mathrm{CWSI}_i - \bar{K}_s\_\mathrm{CWSI}_i)}{\sqrt{\sum_{i=1}^{n}(K_{s,i} - \bar{K}_{s,i})^2 \sum_{i=1}^{n}(K_s\_\mathrm{CWSI}_i - \bar{K}_s\_\mathrm{CWSI}_i)^2}} \geq 0.5. \quad (18)$$

Minimize

$$\mathrm{MAE} = \frac{\sum_{i=1}^{n}\left|K_{s,i} - K_s\_CWSI_i\right|}{n}, \quad (19)$$

where n is the total number of observations, $\grave{K}_{s,i}$ and $\grave{K}_s$_CWSI$_i$ are the daily mean value of water stress from the soil water balance model and from the CWSI, respectively.

Uncertainty of TAW$_r$ and its influence on crop transpiration

After the optimal TAW$_r$ from CWSI was obtained from the above iterative procedure (Fig. 3), the Markov chain Monte Carlo (MCMC) method with Metropolis Hastings sampling algorithm was applied to determine the probability distribution of TAW$_r$ parameters. The output from MCMC provides a set of acceptable TAW$_r$ parameters values, which captures the probabilistic certainty of TAW$_r$ parameters in light of the observed crop water stress coefficient (K_s_CWSI). The accepted TAW$_r$ parameter set could be used to determine the probability distribution and uncertainty of estimated TAW$_r$. Additional details of the MCMC algorithm are described in Gelman et al. (2013). For this study, the MCMC technique using one chain for each treatment in 3 years was implemented, and each chain consisted of 3000 acceptable samples of TAW$_r$. To accelerate the convergence of the MCMC chain, the obtained optimized TAW$_r$ was used as the starting point for each MCMC chain. The first 1500 acceptable samples of TAW$_r$ were treated as a "burn in" period and were discarded (Gelman et al. 2013; Hartig et al. 2012). Thus, a total of 1500 acceptable samples of TAW$_r$ were obtained for each treatment across 3 years, and were used to determine parameter probability distributions. The "metrop" function in R "mcmc" package was used for above MCMC application (Geyer and Johnson 2015).

To study the impact of TAW$_r$ on crop transpiration under different irrigation levels, a scenario (sensitivity) study was carried out. Three irrigation levels and five TAW$_{max}$ levels (120, 100, 90, 80, 70 mm) were considered. The three irrigation levels, TR1 (100/100), TR8 (65/65) and TR12 (40/40) were chosen to represent different conditions of water availability, including well-watered condition (STR 1), medium water availability condition (STR8), and severe deficit condition (STR12) in 2015. The input of water balance model (except TAW$_{max}$ and irrigation schedule) for TR1 in 2015 was used for this scenario study, and the model was run fifteen times with different levels of irrigation and TAW$_{max}$. The impact of TAW$_{max}$ on crop transpiration under different irrigation levels at daily and seasonal scales was studied.

Evaluation of optimized TAW$_r$

To evaluate the performance of the optimized TAW$_r$ method on the soil water deficit prediction, the soil water balance model, with the optimized TAW$_r$ (Model-TAW$_r$), was compared with the observed soil water deficit. In addition, for comparison purposes, another simulation scenario was used running the water balance model using empirical parameters, 7, 68, 20.25, and 120 mm for t_1, t_x, TAW$_{min}$, TAW$_{max}$, respectively (Model-FAO). These parameters were set based on soil texture, the rooting depth and crop growth stage measurements. Root Mean square error (RMSE), Nash–Sutcliffe coefficient (Nash), and mean absolute error (MAE) were used to evaluate the goodness of model simulation (Nash and Sutcliffe 1970; Willmott 1982).

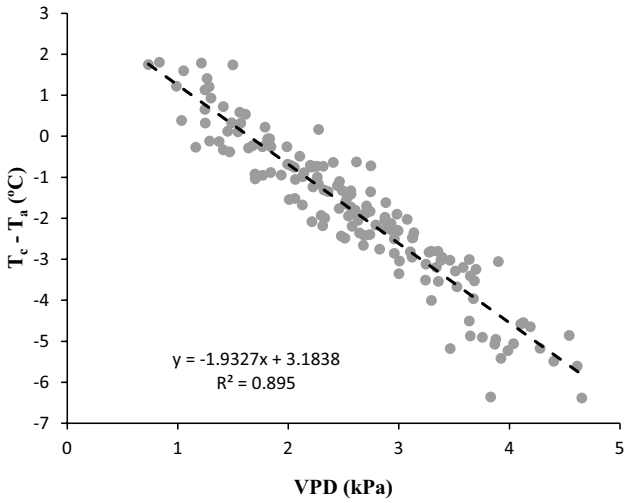

Fig. 4 Non-water stress baseline developed in this study with observations from the full irrigation treatment in 2012, 2013 and 2015 ($T_c - T_a = b \times \mathrm{VPD} + a$; dash line and gray dots)

Results and discussion

Calculated CWSI

A strong negative correlation between VPD and $T_c - T_a$ (p value < 0.001) was found with data from 3 years (Fig. 4). The coefficients of non-stress baseline are shown in Fig. 4, and calculated seasonal average r_a and r_{cp} were 11.55 (s m^{-1}) and 38.88 (s m^{-1}), respectively. The coefficients for the baseline were similar to those obtained by previous studies in Greeley, Colorado (DeJonge et al. 2015; Taghvaeian et al. 2014b), where the slope "b" ranged from − 1.79 to − 2.0, and the intercept "a" ranged from 2.3 to 3.4 for maize in this region. Results obtained in this study are reasonable, since other studies reported similar values. The average resistances obtained by O'Toole and Real (1986) obtained were r_a of 14.9 s m^{-1} and r_{cp} of 56.3 s m^{-1}. Jackson et al. (1981) stated that it was reasonable to use a constant r_a, around 6–10 m s^{-1}. Tolk (1992) reported the values of r_{cp} ranging from 30 to approximately 110 s m^{-1} during the corn growing season. Thus, the parameters (r_a and r_{cp}) obtained for CWSI in this study are reasonable.

Average CWSI values by growth stage in each year are shown in Table 4. In the late vegetative stage, CWSI responded to the water stress created by the treatments. When crops entered the reproductive stage, full irrigation was resumed for all treatments and all CWSI values decreased to between 0 and 0.2. When crops reached the maturity stage, CWSI values increased again in those treatments in which deficit irrigation was resumed. For TR13 (40/80), more water was applied during the maturation stage than the vegetation stage in 2015. Therefore, CWSI value for

Table 4 Seasonal average CWSI for different crop growth stage in 3 years (*TR* treatment, *Veg* vegetative stage, *Rep* reproductive stage, *Mat* maturation stage)

Year	Growth stage	TR1 100/100	TR2 100/50	TR3 80/80	TR6 80/40	TR7 65/80	TR8 65/65	TR9 65/50	TR10 65/40	TR11 50/50	TR12 40/40	TR13 40/80
2012	Veg	0.14	0.15		0.13		**0.24**		**0.23**		*0.41*	
	Rep	0.08	0.03		0.05		0.11		0.12		0.12	
	Mat	0.17	**0.32**		**0.32**		**0.27**		**0.37**		**0.27**	
2013	Veg	0.12	0.09		0.10		0.19				*0.45*	
	Rep	0.03	0.05		0.05		0.03				0.07	
	Mat	0.12	**0.30**		*0.47*		0.18				*0.49*	
2015	Veg	0.09	0.09	**0.20**			**0.37**	*0.43*	*0.25*	*0.45*	*0.55*	*0.58*
	Rep	0.07	0.07	0.09			0.16	0.13	0.11	0.14	0.16	0.19
	Mat	**0.20**	*0.49*	**0.36**			*0.55*	*0.64*	*0.64*	*0.64*	*0.68*	**0.39**

Values greater than 0.2 indicate moderate stress and are in bold, values greater than 0.4 indicate major stress and are italic

Table 5 Statistical analysis of modeled and observed soil water deficit (mm) by different scenarios

Year	Treatment	Nash		RMSE		MAE	
		Model-FAO	Model-TAW	Model-FAO	Model-TAW	Model-FAO	Model-TAW
2012	TR1 (100/100)	0.15	-0.02	16.10	17.63	13.16	14.84
	TR2 (100/50)	0.88	0.86	9.99	10.65	8.34	8.58
	TR6 (80/40)	0.87	0.79	11.37	14.77	9.71	12.45
	TR8 (65/65)	0.43	0.77	16.00	10.13	14.16	8.31
	TR10 (65/40)	0.56	0.81	16.73	10.93	15.18	8.67
	TR12 (40/40)	0.49	0.60	16.28	14.44	15.34	13.36
2013	TR1 (100/100)	− 0.50	0.29	21.54	14.88	17.76	11.21
	TR2 (100/50)	0.20	0.51	20.71	16.19	17.62	13.09
	TR6 (80/40)	− 0.46	0.29	28.66	19.96	24.86	17.18
	TR8 (65/65)	− 0.23	0.61	22.73	12.78	20.03	9.96
	TR12 (40/40)	0.45	0.68	20.00	15.10	17.61	12.14
2015	TR1 (100/100)	0.48	0.34	12.84	14.53	9.95	11.18
	TR2 (100/50)	0.72	0.82	15.71	12.54	12.80	10.09
	TR3 (80/80)	0.30	0.58	15.74	12.18	12.49	9.30
	TR8 (65/65)	− 1.03	0.06	27.37	18.63	19.94	14.10
	TR9 (65/50)	0.23	0.76	19.50	10.83	16.00	8.90
	TR10 (65/40)	0.88	0.89	10.18	9.86	8.15	7.11
	TR11 (50/50)	0.75	0.82	12.97	10.82	10.25	7.39
	TR12 (40/40)	0.65	0.81	14.44	10.67	11.91	8.95
	TR13 (40/80)	0.27	0.53	19.23	15.40	15.04	11.63

Model-TAW: soil water balance model with optimized TAW_r and K_{cb} estimated from crop coverage. Model-FAO: soil water balance model with experience TAW_r and K_{cb} estimated from FAO document

Nash Nash–Sutcliffe model efficiency coefficient, *RMSD* root-mean-square deviation, *MAE* mean absolute error

TR13 in the maturation stage was lower than that in the vegetative stage. Consequently, calculated CWSI in this study responded well as expected to crop water stress differences between treatments and growth stages.

Soil water deficit

Model-TAW_r resulted in improved estimation of soil water deficit compared to Model-FAO (Table 5; Fig. 5). Using TAW_r estimated from CWSI, the averaged Nash coefficient of all treatments and for all 3 years increased from 0.28 to 0.5; while the averaged RMSE and MAE of all treatments during all 3 years decreased from 14.4 to 17.2 to 11.5 and 14.3 mm, respectively. This means a reduction of the RMSE and MAE by 17 and 20%, respectively, compared with Model-FAO. Model-FAO overestimated soil water deficit, due to overestimation of TAW_r, especially in Treatment 8 (Table 5; Fig. 5). Comparing simulated soil water deficit with Model-TAW_r, it was clear that Model-TAW_r could well-describe the response of soil water deficit to irrigation management in each treatment (Fig. 5). Overall, the soil water deficit estimated by Model-TAW_r was reasonable for all treatments in all 3 years. Using the TAW_r estimated from CWSI, the model was able to improve water deficit estimation.

Optimized parameters and uncertainty

The optimized parameters for Model-TAW_r through the iterative process are shown in Table 6. The optimized soil water balance model using the CWSI approach seemed to yield a reasonable value for the TAW_r, compatible with the empirical values from field measurements. The average value of the field estimated field capacity in this experimental field was 0.20–0.24 $m^3\ m^{-3}$. The root length distribution in the experiment field varied considerably between treatments. For deficit irrigation treatments, deeper root systems were found than for the full irrigation treatment (Comas et al. 2013). The observed maximum rooting depth varied from 800 mm to 1050 mm in year 2012. It is common for maize irrigation to assume that the soil volumetric water content at wilting point is 50% of field capacity (Allen et al. 1998; DeJonge et al. 2015). Thus, the estimated maximum TAW_r from experimental data ($TAW_r - E$) ranged from 80 mm ($0.20 \times 800 \times 0.5$) to 126 mm ($0.24 \times 1050 \times 0.5$). As shown in Table 6, most of CWSI derived maximum TAW_r values were within the range of $TAW_r - E$. Furthermore, the CWSI

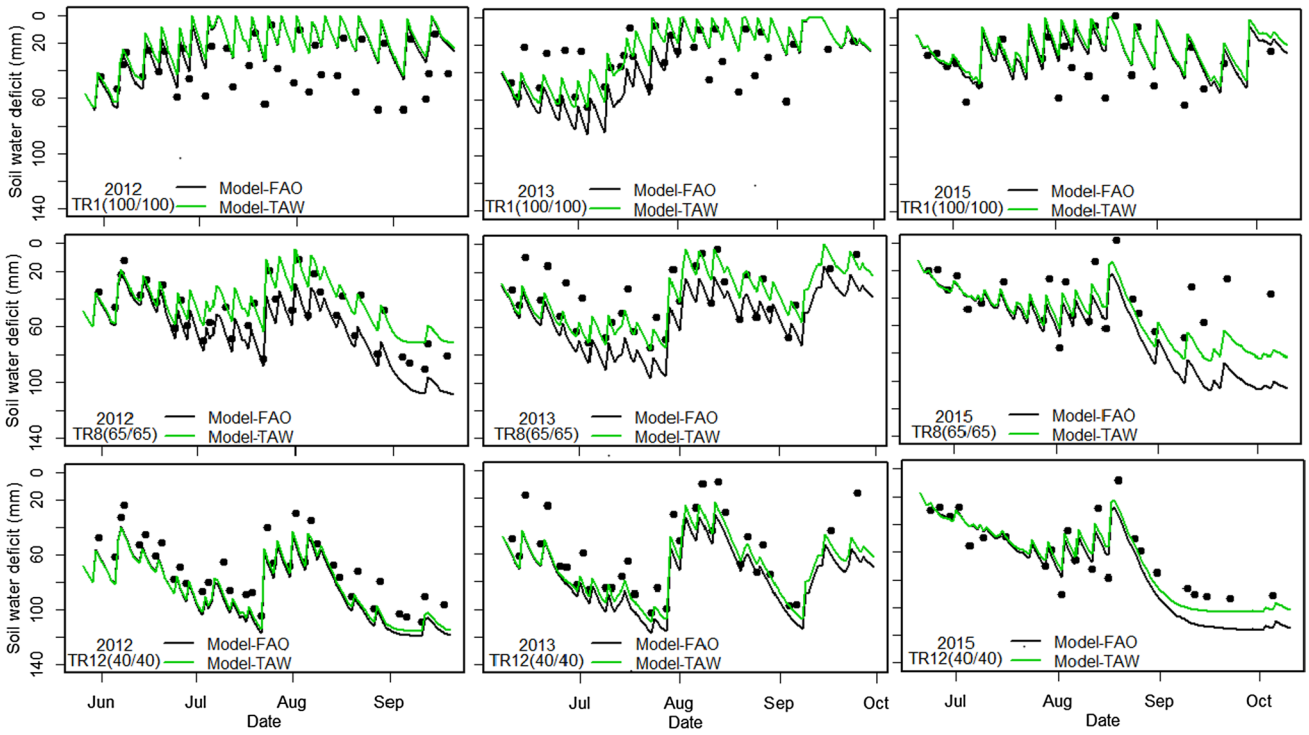

Fig. 5 Comparing simulated daily soil water deficit by Model-TAW and Model-FAO, with measured soil water deficit (black points) in 2012, 2013 and 2015. Model-FAO is the water balance model with estimated TAWr from experiment. Model-TAW is the water balance model with estimated TAWr from canopy temperature. *RAWr* is the readily available water in the root zone, and TAWr is the total available water in the root zone. See Table 1 for TR1 (100/100), TR8 (65/65), TR10 (65/40) and TR12 (40/40)

Table 6 Optimized parameters and their 95% confidence interval (in parentheses) for TAW_r parameters

Year	Treatment	t_1	t_x	TAW_{max}	TAW_{min}
2012	TR1 (100/100)	15.6 (6.0, 20.0)	54.3 (50.2, 70.0)	76.7 (70.1, 77.0)	18.1 (18.0, 22.0)
	TR2 (100/50)	16.1 (6.0, 16.1)	62.9 (50.0, 64)	89.3 (88.8, 91.3)	19 (18.0, 22.0)
	TR6 (80/40)	12.8 (6.0, 15.7)	56.5 (50.0, 66.8)	104.9 (103.3, 110.7)	18.2 (18.0, 20.3)
	TR8 (65/65)	13.3 (6.0, 20.0)	67.8 (52.0, 70.0)	71.3 (70.0, 79.0)	19.8 (18.0, 21.7)
	TR10 (65/40)	12.6 (6.0, 16.5)	62.9 (50.0, 58.6)	104.4 (99.4, 104.1)	18.6 (18.0, 20.5)
	TR12 (40/40)	17.2 (6.0, 20.0)	68.7 (66.0, 70.0)	116.3 (111.1, 127.1)	20.6 (18.0, 22.0)
2013	TR1 (100/100)	17.3 (6.0, 20.0)	56.1 (50.3, 59.9)	72.5 (70.0, 84.5)	18.1 (18.0, 21.6)
	TR2 (100/50)	17.5 (6.0, 20.0)	54.6 (50.1, 61.7)	82.1 (72.2, 84.2)	18.1 (18.0, 21.0)
	TR6 (80/40)	14.2 (11.0, 20.0)	59.4 (50.5, 57.0)	93.4 (92.6, 97.2)	18.3 (18.0, 19.7)
	TR8 (65/65)	18.6 (14.3, 20.0)	67.1 (60.0, 70.0)	89.1 (85.2, 96.6)	18.4 (18.0, 20.4)
	TR12 (40/40)	11.4 (12.9, 19.9)	69.3 (69.1, 70.0)	110.8 (97.7, 107)	19.9 (18.0, 22.0)
2015	TR1 (100/100)	18.7 (6.6, 19.1)	50.6 (51.3, 69.9)	85 (70.0, 86.9)	18.4 (18, 22.0)
	TR2 (100/50)	12.2 (6.2, 19.8)	54.5 (50.0, 60.1)	95.7 (94.5, 102.3)	21.9 (18, 22.0)
	TR3 (80/80)	12.4 (6, 19.1)	60.1 (50, 65.7)	70.9 (70.1, 82.8)	21.7 (18, 22.0)
	TR8 (65/65)	16.1 (12.2, 20.0)	60.1 (50.1, 60.6)	86.5 (83.9, 88.9)	21.6 (18, 22.0)
	TR9 (65/50)	16 (6.1, 20.0)	68.3 (61.3, 70.0)	85.6 (83.4, 86.7)	21.1 (18, 22.0)
	TR10 (65/40)	15.4 (9.4, 20)	64.8 (52.5, 68.3)	108.3 (105.8, 110.8)	20.3 (18, 22.0)
	TR11 (50/50)	15.2 (13.4, 19.9)	66.6 (66.0, 70.0)	93.4 (88.4, 91.7)	20.5 (18.1, 22.0)
	TR12 (40/40)	15.9 (12.3, 19.5)	69.6 (66.6, 70)	103.6 (101.4, 104.7)	21.4 (18.1, 22.0)
	TR13 (40/80)	14.2 (6.0, 18.0)	66.1 (64.5, 70)	72.2 (70.0, 73.4)	20.2 (18.1, 22.0)

t_1, t_x, TAW_{max}, and TAW_{min} are parameters for TAW_r development in Eq. 11

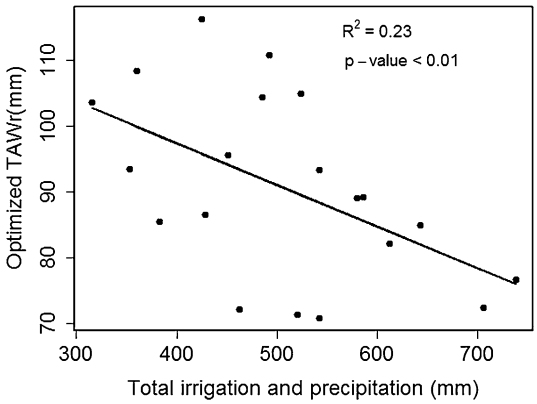

Fig. 6 Relationship between optimized maximum TAW_r and total irrigation and precipitation in 2012, 2013, and 2015

derived TAW_r had a significant relationship with the total irrigation and precipitation amounts during the growing season (Fig. 6). The TAW_r increased with the decrease in the total irrigation and precipitation.

The TAW_r parameter distributions of TR1, TR8 and TR12 are shown in Fig. 7. Normal distributions with narrow ranges are associated with well-quantified parameters, indicating that K_s is sensitive to those parameters. TAW_{max}, which determines the maximum total available water in the root zone, was the most sensitive and best identified parameter. On the other hand, TAW_{min} showed a flat distribution and thus was not well-identified; thus the changing of TAW_{min} had limited impact on K_s. Comparing the distributions of parameters among different treatments, the parameters in deficit treatments TR8 and TR12 were better identified. This

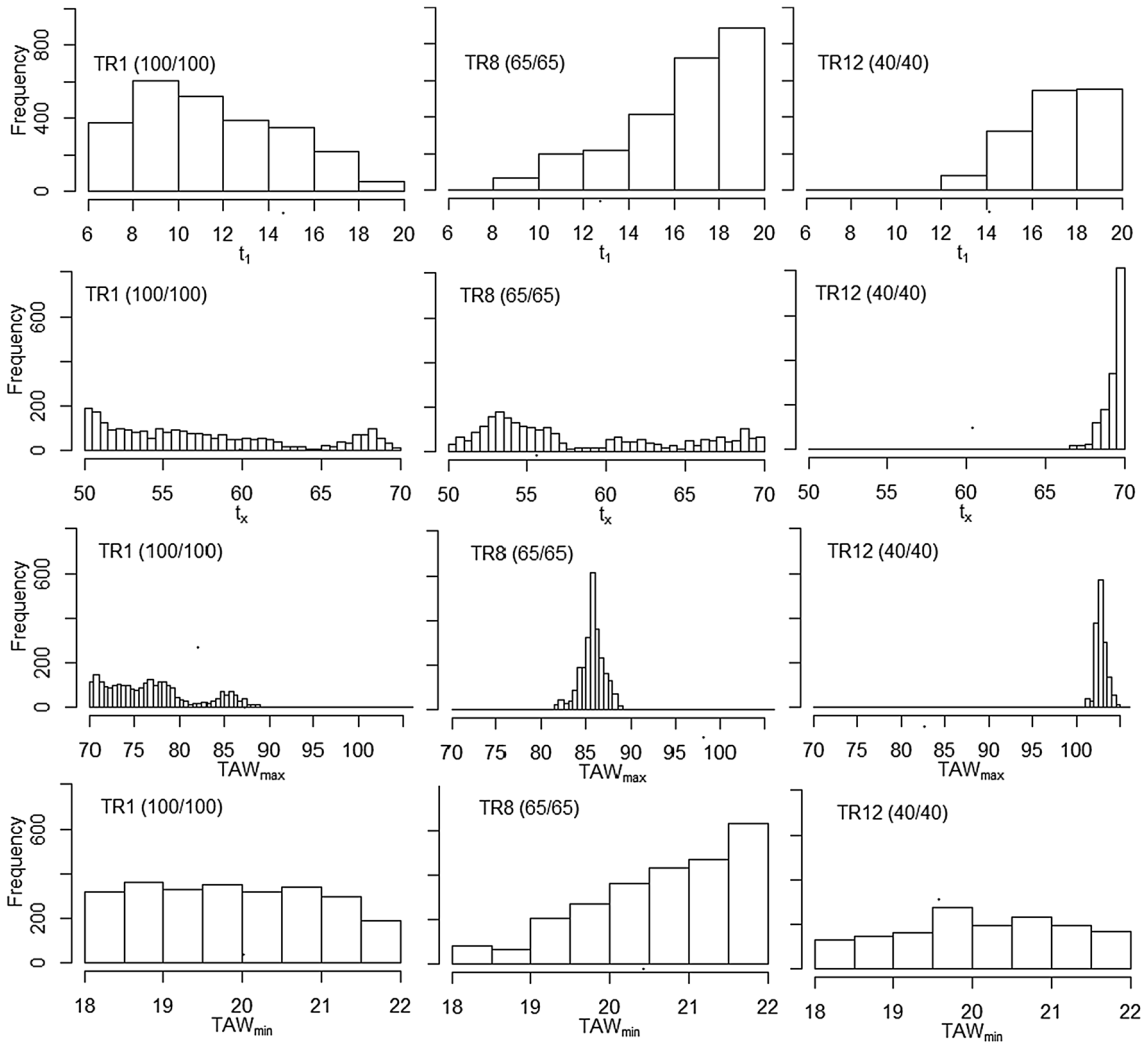

Fig. 7 Probability distributions of TAWr parameters in TR1 (100/100), TR8 (65/65) and TR12 (40/40) in 2015

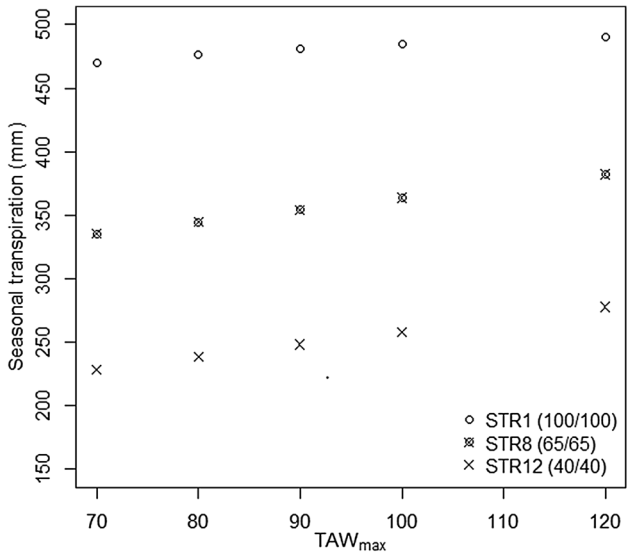

Fig. 8 Impact of TAW_{max} on crop seasonal transpiration with three irrigation levels in 2015. STR1-scenario with irrigation schedule of TR1 (100/100), STR8-scenario with irrigation schedule of TR8 (65/65), STR12- scenario with irrigation schedule of TR12 (40/40)

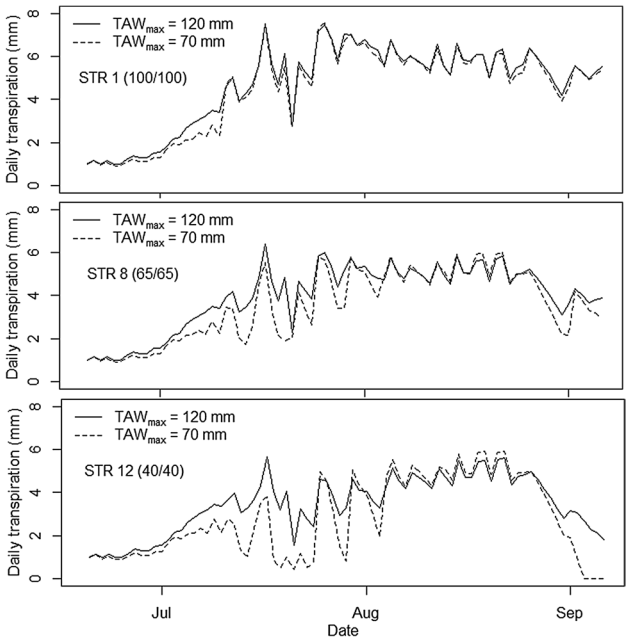

Fig. 9 Impact of TAW_{max} on crop daily transpiration with three irrigation levels in 2015e. STR1- scenario with irrigation schedule of TR1 (100/100), STR8-scenario with irrigation schedule of TR8 (65/65), and STR12-scenario with irrigation schedule of TR12 (40/40)

result may indicate that the irrigation level has an impact on estimating TAW_r using the CWSI approach.

The actual TAW_r is difficult to measure in the field due to variability of soil texture and crop rooting depth. Estimates of TAW_r estimated from CWSI were reasonable, because the variation of the TAW_r (derived from CWSI) between treatments could be explained by the total irrigation and precipitation and because it improved the soil water balance model (SWDr) prediction as reported in Table 5.

Impact of TAW_{max} on transpiration under different irrigation levels

The impact of TAW_{max} on seasonal transpiration with different irrigation levels is shown in Fig. 8. Seasonal transpiration decreases with the decreasing TAW_{max} and irrigation amounts, due to reduced soil water holding capacity. The reduction in seasonal transpiration between TAW_{max} values of 120 and 70 mm was 19, 54 and 55 mm, or by 4, 14 and 21% for STR1, STR8 and STR12, respectively. The slopes of the decreasing trend between TAW_{max} and seasonal transpiration were 0.39, 0.93 and 0.98 for STR1, STR8 and STR12, respectively. Thus, TAW_{max} has little impact on seasonal transpiration in well-watered scenarios, but it has a strong impact on seasonal transpiration under deficit irrigation and water stress conditions. The impact of TAW_{max} on daily transpiration with different irrigation level is shown in Fig. 9. The change of daily transpiration caused by TAW_{max} was small in the well-watered scenario and during well-irrigated periods (8/3/2015–8/23/2015), and it was substantial under deficit irrigation conditions. This explains the lack of improvement using Model-TAW and lower estimated TAW_{max} for treatment TR1 (100/100) (Tables 5, 6; Fig. 7). The optimization procedure could not find the reasonable TAW_{max} values in TR1, since the change of TAW_{max} does not substantially influence the crop transpiration or crop water stress index for the fully watered crops.

Applications and limitations

Currently, multispectral remote sensing observations of canopy characteristics are available from various platforms, such as satellite, airborne, unmanned aerial vehicles, as well as ground-based systems. These remote sensing data have widely been used to estimate instantaneous (hourly) actual ET and crop water stress indices (Allen et al. 2007; Colaizzi et al. 2012; Sayago et al. 2017). Except for the measurements from IRT sensors, other remote sensing measurements have relatively low temporal resolution to provide continuous actual ET and crop water stress estimations due to low revisit frequency (temporal resolution) or cloud cover condition. Various hydrologic and agricultural system models are able to provide continuous ET and water stress estimations. However, most applications of these models used estimated or assume TAWr value that can only be validated by developing hydrographs at river-basin outlets (large scale water balance) or using intensive soil water content measurements.

Thus, there is limited confidence on the accuracy of actual ET predicted by these models. In this study, the proposed framework couples the CWSI (from canopy temperature measurements) and the FAO soil water balance model to provide more accurate and continuous actual ET and soil water deficit estimations. The CWSI in the proposed framework could be replaced by actual ET values estimated from multispectral remote sensing data, because actual ET is also regulated by *TAWr*. The FAO water balance model could be replaced with other hydrologic models such as SWAT model.

Compared with other studies that tried to assimilate ET from remote sensing and ET from FAO-56 model simulation (Er-Raki et al. 2008; Neale et al. 2012), the proposed approach does not need previous knowledge of TAW_r and thus may be more applicable when root development and soil textures are not available. At the same time, the data assimilation approach presented in (Er-Raki et al. 2008; Neale et al. 2012) only change the modeled ET when remotely sensed ET is available. The proposed framework used discontinuous remotely sensed measurements to determine the TAWr curve. Then, the TAWr curve regulates modeled ET during the whole growing season. Therefore, this framework may provide a solution or an alternative to the knowledge gap regarding estimating TAW using remote sensing data; which is not solved by data assimilation approaches.

The limitation of the proposed framework is that it requires remote sensing measurements of canopy temperature under crop water stress conditions. The TAWr estimation (as proposed in this study) does not apply if the crop is not under soil water stress conditions. The reasons for this limitation could be the large uncertainty in estimated TAWr when all remote sensing measurements are under non-water stress condition (Sect. "Optimized parameters and uncertainty"), and that the change of TAWr has little impact on crop water stress/ET under non-water stress condition (Sect. "Impact of TAW_{max} on transpiration under different irrigation levels").

Conclusions

In this paper, a canopy temperature-based crop water stress index was incorporated into a soil water balance model to determine the total available water in the crop root zone to improve the water balance estimation of soil water deficit (depletion). The statistical analyses indicated that the TAW_r estimated from CWSI significantly improved the estimation of soil water deficit values, which reduced the mean absolute error (MAE) and root mean squared error (RMSE) by 17 and 20%, compared with standard FAO model with experience estimated TAW_r. This result showed that TAW_r estimated using CWSI could significantly improve the performance of the FAO-56 soil water balance model for the estimation of soil water deficit throughout the crop growing season. The proposed procedure applies for deficit irrigated crops, because the change of TAW_{max} does not significantly influence crop transpiration or CWSI without crop stress.

Appendix 1 theoretical calculation of CWSI

The theoretical development of CWSI is based on surface energy balance equation, as the theoretical method uses the surface energy balance equation, whilst accounting for variation in climate, and calculates the divergence between the upper and lower boundaries of the canopy-to-air temperature difference (Jackson et al. 1981, 1988). The temperature difference between canopy and air could be defined as:

$$T_c - T_a = \frac{r_a}{\rho c_p}\frac{\gamma(1 + r_c/r_a)}{\Delta + \gamma(1 + r_c/r_a)}R_n - \frac{e^* - e}{\Delta + \gamma(1 + r_c/r_a)}, \quad (20)$$

where c_p is the heat capacity of air (J kg^{-1} °C), T_c is the temperature of canopy, T_a is the air temperature, e^* is the air saturated vapor pressure at T_c (Pa), e is the air vapor pressure (P_a), γ is the psychrometric constant (Pa $℃^{-1}$), r_a is the aerodynamic resistance (s m^{-1}), r_c is the canopy resistance (s m^{-1}), Δ is the change (slope) of saturation vapor pressure with temperature (Pa $℃^{-1}$), and R_n is the net radiation (J m^{-2} s^{-1}).

Then, the upper boundary of $(T_c - T_a)$ is calculated, when $r_c \rightarrow \infty$:

$$(T_c - T_a)_u = \frac{\bar{r}_a}{\rho c_p}R_n. \quad (21)$$

And, the lower boundary of $(T_c - T_a)$ is calculated, when $r_c = r_{cp}$

$$(T_c - T_a)_l = \frac{r_a}{\rho c_p}\frac{\gamma(1 + \bar{r}_{cp}/\bar{r}_a)}{\Delta + \gamma(1 + \bar{r}_{cp}/\bar{r}_a)}R_n - \frac{e^* - e}{\Delta + \gamma(1 + \bar{r}_{cp}/\bar{r}_a)}, \quad (22)$$

where r_{cp} is the canopy resistance under full transpiration condition.

Many studies have shown that using seasonal average aerodynamic resistance and canopy resistance could give reasonable CWSI value (Clawson et al. 1989; Jalali-Farahani et al. 1993). Here, the aerodynamic and canopy resistances were determined by (O'Toole and Real 1986):

$$\bar{r}_a = \frac{\rho c_p a}{\bar{R}_n b(\bar{\Delta} + 1/b)}, \quad (23)$$

$$\bar{r}_{cp} = -\bar{r}_a\left(\frac{\bar{\Delta} + 1/b}{\gamma} + 1\right), \quad (24)$$

where a and b are the linear regression parameters of the non-water stress baseline of VPD and $T_c - T_a$ (Clawson et al. 1989; O'Toole and Real 1986), R_n is the seasonal average net radiation, Δ is the seasonal average slope of saturated vapor pressure–temperature relationship (Pa ℃$^{-1}$), which is determined by seasonal average mean temperature.

References

Allen RG, Pereira LS (2009) Estimating crop coefficients from fraction of ground cover and height. Irrig Sci 28:17–34

Allen RG, Pereira LS, Raes D, Smith M (1998) Crop evapotranspiration-Guidelines for computing crop water requirements-FAO Irrigation and drainage paper 56. FAO, Rome

Allen RG, Tasumi M, Tressa R (2007) Satellite-based energy balance for mapping evapotranspiration with internalized calibration (METRIC): applications. J Irrig Drain E 133:395–406

Bryla DR, Trout TJ, Ayars JE (2010) Weighing lysimeters for developing crop coefficients and efficient irrigation practices for vegetable crops. HortScience 45:1597–1604

Campos I, González-Piqueras J, Carrara A, Villodre J, Calera A (2016) Estimation of total available water in the soil layer by integrating actual evapotranspiration data in a remote sensing-driven soil water balance. J Hydrol 534:427–439

Clawson K, Jackson R, Pinter P (1989) Evaluating plant water stress with canopy temperature differences. Agron J 81:858–863

Colaizzi PD, Barnes EM, Clarke TR, Choi CY, Waller PM (2003) Estimating soil moisture under low frequency surface irrigation using crop water stress index. J Irrig Drain E 129:27–35

Colaizzi PD, Kusta WP, Anderson MC, Agam N, Tolk JA, Evett SR, Howell TA, Gowda PH, O'Shaughnessy SA (2012) Two-source energy balance model estimates of evapotranspiration using component and composite surface temperatures. Adv Water Resour 50:134–151

Comas LH, Becker SR, Von Mark VC, Byrne PF, Dierig DA (2013) Root traits contributing to plant productivity under drought. Front Plant Sci 4:4–442

Crow WT, Kustas WP, Prueger JH (2008) Monitoring root-zone soil moisture through the assimilation of a thermal remote sensing-based soil moisture proxy into a water balance model. Remote Sens Environ 112:1268–1281

DeJonge KC, Taghvaeian S, Trout TJ, Comas LH (2015) Comparison of canopy temperature-based water stress indices for maize. Agric Water Manag 156:51–62

Er-Raki S, Chehbouni A, Guemouria N, Duchemin B, Ezzahar J, Hadria R (2007) Combining FAO-56 model and ground-based remote sensing to estimate water consumptions of wheat crops in a semi-arid region. Agric Water Manag 87:41–54

Er-Raki S, Chehbouni A, Hoedjes J, Ezzahar J, Duchemin B, Jacob F (2008) Improvement of FAO-56 method for olive orchards through sequential assimilation of thermal infrared-based estimates of ET. Agric Water Manag 95:309–321

Fereres E, Soriano MA (2007) Deficit irrigation for reducing agricultural water use. J Exp Bot 58:147–159

Geli HM (2012) Modeling spatial surface energy fluxes of agricultural and riparian vegetation using remote sensing. Utah State University, Logan

Gelman A, Carlin JB, Stern HS, Dunson DB, Vehtari A, Rubin DB (2013) Bayesian data analysis. CRC press, Boca Raton

Geyer CJ, Johnson LT (2015) Package 'mcmc'. https://cran.r-project.org/web/packages/mcmc/mcmc.pdf. Accessed 3 Oct 2016

Hartig F, Dyke J, Hickler T, Higgins SI, O'Hara RB, Scheiter S, Huth A (2012) Connecting dynamic vegetation models to data—an inverse perspective. J Biogeogr 39:2240–2252

Hsiao TC, Heng L, Steduto P, Rojas-Lara B, Raes D, Fereres E (2009) AquaCrop—the FAO crop model to simulate yield response to water: III. Parameterization and testing for maize. Agron J 101:448–459

Hunsaker DJ, Pinter PJ, Barnes EM, Kimball BA (2003) Estimating cotton evapotranspiration crop coefficients with a multispectral vegetation index. Irrig Sci 22:95–104

Hunsaker DJ, Pinter PJ, Kimball BA (2005) Wheat basal crop coefficients determined by normalized difference vegetation index. Irrig Sci 24:1–14

Idso SB, Jackson RD, Pinter PJ, Reginato RJ, Hatfield JL (1981) Normalizing the stress-degree-day parameter for environmental variability. Agric Meteorol 24:45–55

Irmak A, Kamble B (2009) Evapotranspiration data assimilation with genetic algorithms and SWAP model for on-demand irrigation. Irrig Sci 28:101–112

Jackson RD, Idso SB, Reginato RJ, Pinter PJ (1981) Canopy temperature as a crop water stress indicator. Water Resour Res 17:1133–1138

Jackson RD, Kustas WP, Choudhury BJ (1988) A reexamination of the crop water stress index. Irrig Sci 9:309–317

Jalali-Farahani H, Slack DC, Kopec DM, Matthias AD (1993) Crop water stress index models for Bermudagrass turf: a comparison. Agron J 85:1210–1217

Jensen ME, Allen RG (2016) Evaporation, evapotranspiration, and irrigation water requirements. In: ASCE manual of practice, no. 70, 2nd Ed. ASCE, Reston, VA. https://doi.org/10.1061/9780784414057

Jensen ME, Robb DC, Franzoy CE (1970) Scheduling irrigations using climate-crop-soil data. Proc Am Soc Civil Eng J Irrig Drain Div 96:25–38

Kite GW, Droogers P (2000) Comparing evapotranspiration estimates from satellites, hydrological models and field data. J Hydrol 229:3–18

Kullberg EG, DeJonge KC, Chávez JL (2016) Evaluation of thermal remote sensing indices to estimate crop evapotranspiration coefficients. Agric Water Manag 179:64–73

Mersmann O, Trautmann H, Steuer D, Bischl B, Deb K (2014) Package "mco": multiple criteria optimization algorithms and related functions. https://cran.r-project.org/web/packages/mco/mco.pdf. Accessed 3 Oct 2016

Nash JE, Sutcliffe JV (1970) River flow forecasting through conceptual models part I—a discussion of principles. J Hydrol 10:282–290

Neale CM, Bausch WC, Heermann DF (1990) Development of reflectance-based crop coefficients for corn. Trans ASAE 32:1891–1900

Neale CMU et al (2012) Soil water content estimation using a remote sensing based hybrid evapotranspiration modeling approach. Adv Water Resour 50:152–161

O'Toole J, Real J (1986) Estimation of aerodynamic and crop resistances from canopy temperature. Agron J 78:305–310

Pereira LS, Oweis T, Zairi A (2002) Irrigation management under water scarcity. Agric Water Manag 57:175–206

Raes D, Geerts S, Kipkorir E, Wellens J, Sahli A (2006) Simulation of yield decline as a result of water stress with a robust soil water balance model. Agric Water Manag 81:335–357

Rallo G, Agnese C, Minacapilli M, Provenzano G (2011) Comparison of SWAP and FAO agro-hydrological models to schedule irrigation of wine grapes. J Irrig Drain E 138:581–591

Santos C, Lorite IJ, Tasumi M, Allen RG, Fereres E (2008) Integrating satellite-based evapotranspiration with simulation models for irrigation management at the scheme level. Irrig Sci 26:277–288

Sayago S, Ovando G, Bocco M (2017) Landsat images and crop model for evaluating water stress of rainfed soybean. Remote Sens Environ 198:30–39

Steduto P, Hsiao TC, Raes D, Fereres E (2009) AquaCrop—the FAO crop model to simulate yield response to water: I. Concepts and underlying principles. Agron J 101:426–437

Taghvaeian S, Chávez JL, Bausch WC, DeJonge KC, Trout TJ (2014a) Minimizing instrumentation requirement for estimating crop water stress index and transpiration of maize. Irrig Sci 32:53–65

Taghvaeian S, Comas L, DeJonge KC, Trout TJ (2014b) Conventional and simplified canopy temperature indices predict water stress in sunflower. Agric Water Manag 144:69–80

Tolk JA (1992) Corn aerodynamic and canopy surface resistances and their role in sprinkler irrigation efficiency. Texas Tech University, Lubbock

Toureiro C, Serralheiro R, Shahidian S, Sousa A (2017) Irrigation management with remote sensing: evaluating irrigation requirement for maize under Mediterranean climate condition. Agric Water Manag 184:211–220

Trout TJ, Johnson LF, Gartung J (2008) Remote sensing of canopy cover in horticultural crops. HortScience 43:333–337

Willmott CJ (1982) Some comments on the evaluation of model performance. Bull Am Meteorol 63:1309–1313

Zhang H, Wang D (2013) Management of postharvest deficit irrigation of peach trees using infrared canopy temperature. Vadose Zone J 12(3). https://doi.org/10.2136/vzj2012.0093